

Figure S1. (A) Gleason scores of the 550 patients analyzed based on the GLI1/IFT20 signature extracted from the TCGA PRAD database. (B) Volcano plot of the distribution of all differentially expressed genes based on the GLI1⁺/IFT20⁺ ciliated cells *versus* non ciliated cell signature (GLI1⁺/IFT20⁻, GLI1⁻/IFT20⁻, GLI1⁻/IFT20⁺). (C) KEGG pathway enrichment of genes downregulated in GLI1⁺/IFT20⁺ prostate tumors (TCGA-PRAD). Bar plot showing the top KEGG pathways enriched among genes significantly downregulated in the 5 % of prostate cancer patients from the TCGA-PRAD dataset co-expressing GLI1 and IFT20. This subgroup also exhibits strong overexpression of Synaptophysin (SYP), repression of RB1, and a trend toward increased YAP1 expression. The most significantly enriched pathway is oxidative phosphorylation. For each pathway, the Gene Ratio (proportion of input genes involved in the pathway) and the adjusted p-value (p.adjust) are indicated (D) Reactome pathway enrichment of genes downregulated in GLI1⁺/IFT20⁺ prostate tumors (TCGA-PRAD). Bar plot showing the top enriched Reactome pathways among genes significantly downregulated in the 5 % of prostate cancer patients from the TCGA-PRAD dataset co-expressing GLI1 and IFT20. The most significantly enriched pathway is Respiratory electron transport. For each pathway, the Gene Ratio (proportion of input genes involved in the pathway) and the adjusted p-value (p.adjust) are indicated (E) GO Biological Process enrichment of genes downregulated in GLI1⁺/IFT20⁺ prostate tumors (TCGA-PRAD). Bar plot showing the top enriched GO biological processes among genes significantly downregulated in the 5 % of prostate cancer patients co-expressing GLI1 and IFT20. The most enriched terms include mitochondrial ATP synthesis coupled electron transport, aerobic respiration, and oxidative phosphorylation. (F) Schematic representation of the different zones used in localized patients (normal zone, peritumoral zone and tumoral zone) and in CRPC patients (tumoral zone). Created in <https://BioRender.com>. (G) Axial CT scan (non-contrast) from patients 1, 2, 3 and 5 from Antoine Lacassagne Center.

Figure S2. (A-C) Representative immunofluorescence of patients 2 (A), 3 (B), 4 (C) and 5 (D) from Centre Antoine Lacassagne. Immunofluorescence labeled with Pericentrin (green), Arl13b (red), panNE (yellow), panCK (grey) and DAPI (blue). Samples were studied to evaluate the prediction model of the absence or presence of the PC in a putative NE zone.

Figure S3. (A) Positive control condition showing nuclear staining with DAPI (blue) and robust expression of the proliferation marker KI67 (yellow), confirming correct KI67 detection. Co-staining with pan-cytokeratin (pan-CK) identifies proliferating epithelial cells. (B) Immunofluorescence analysis of CRPC patient tumor sections, stained for ARL13B (red), Pericentrin (green), KI67 (yellow) and DAPI (blue), with pan-NE marking neuroendocrine tumor areas. Higher-magnification views highlight NE cell regions lacking KI67 expression.

Figure S4. (A) Cell lysates from P69 cells exposed to hypoxia (Hx 1%) treated 48h with Gefitinib (Gef. 10 μ M) were analyzed by immunoblot using HIF-1 α protein, along with β -tubulin as loading control. Immunoblot (inset) and quantification of HIF-1 α expression. (B) Quantification of the transcriptional expression of CPT1 obtained through RT-qPCR conducted on P69 cells treated with 100 μ M of Clofibrate. (C) Quantification of the percentage of ciliated cells in P69 cell treated with Gefitinib (10 μ M) and Clofibrate (100 μ M) in hypoxia (Hx – 1% O₂) for 48h (n>250). (D) Cell viability of NCI-H660 cells cultured under normoxic (Nx) or hypoxic (Hx 1%)

conditions for 3 days (D3) and 6 days (D6). (E) Immunofluorescence of LNCaP, DU145 and PC3 cells exposed to normoxia (Nx) and hypoxia (Hx – 1% O₂) for 72h and labeled with acetylated α -tubulin (acetylated α -tub.) (red) and Arl13b (green) along with DAPI (blue) (magnification: x60, scale bar 10 μ m). (F) Cell lysates from DU145 and PC3 cells exposed to hypoxia (Hx 1%) treated 48h with Gefitinib (Gef. 10 μ M) were analyzed by immunoblot using HIF-1 α protein, along with β -tubulin as loading control. Quantification of HIF-1 α expression. (G-H) Quantification of the transcriptional expression of CPT1 obtained through RT-qPCR conducted on DU145 (G) and PC3 (H) cells treated with 100 μ M of Clofibrate. (I) Quantification of the percentage of ciliated cells in DU145 cells treated with Gefitinib (10 μ M) and Clofibrate (100 μ M) in normoxia (Nx) and hypoxia (Hx) for 48h (n>250). (J) Quantification of the percentage of ciliated cells in PC3 cells treated with Gefitinib (10 μ M) and Clofibrate (100 μ M) in normoxia (Nx) and hypoxia (Hx) for 48h (n>250).

All quantifications were performed using GraphPrism9 software. Statistical analysis: Two-way ANOVA; significant differences are indicated by * p<0.05 and ** p<0.005.

Figure S5. (A) Boyden chamber trans-well migration assay with LNCaP-shCtl and LNCaP-shYAP1 cells on collagen coated membranes with 8 μ m porosity. Counts were performed after 24h. (B) Boyden chamber trans-well migration assay with DU145-shCtl and DU145-shYAP1 cells on collagen coated membranes with 8 μ m porosity. Counts were performed after 24h. (C) Cell lysates from PC3 transfected with siYAP or not (siCtl) were analyzed by immunoblot using YAP1 protein, along with β -tubulin as loading control. (D) Immunofluorescence of PC3 cells transfected with siCtl or siYAP1 and labeled with YAP1 (red) (magnification: x60, scale bar 10 μ m). (E) Boyden chamber trans-well migration assay with PC3 transfected with a siCtl or siYAP1 cells on collagen coated membranes with 8 μ m porosity. Counts were performed after 24h. (F) Immunofluorescence of PC3 cells transfected with siCtl or siYAP1 and labeled with Pericentrine (green), ARL13B (red) and DAPI (blue) (magnification: x60, scale bar 10 μ m). (G) Cell lysates from PC3 transfected with siYAP1, siTAZ, siYAP1/TAZ or control siRNA (siCtl) were analyzed by immunoblot using YAP1 and TAZ proteins, along with ERK2 as loading control. (H) Cell lysates from PC3 transfected with siYAP or not (siCtl) were analyzed by immunoblot using SYP protein, along with β -tubulin as loading control. Cell lysates from NCI-H660 were used as control. (I) Quantification of Notch4 (Notch receptor) transcript levels in (i) LNCaP cells untreated (-) or treated with enzalutamide (+), (ii) DU145 shCtl (-) or shYAP1 (+), (iii) PC3 untreated (-) or treated with Jasplakinolide (Jasp.; +) and (iv) NCI-H660 as reference. The presence of the primary cilium (PC) is indicated below each condition: (-) no cilium, (+) <10% ciliated cells, (+++) >50% ciliated cells.

Quantifications shown in panel H were performed using GraphPad Prism 9. Statistical analysis was conducted using two-way ANOVA. Significance is indicated as follows: *p < 0.05, **p < 0.005, ***p < 0.0005, ****p < 0.0001. For all other panels, unpaired two-tailed t-tests were used unless otherwise specified.

Figure S6. (A) Quantification of the transcriptional expression of CCN1 and CCN2 obtained through RT-qPCR conducted on DU145 cells treated for 5d with 1 μ M of Jasplakinolide (Jasp.). (B) Heatmap of differentially expressed genes in PC3 cells treated with Jasplakinolide. Gene expression profiles of PC3 cells treated with 1 μ M Jasplakinolide (Jasp.) were compared to untreated PC3 cells. K-means clustering (Phantasus v1.19.3) identified 11 distinct gene clusters. Among them, five clusters - three with upregulated genes (in red) and two with downregulated genes (in blue) - highlight significant transcriptional changes related to

microtubule organization, centrosome function, and centromeric spindle assembly. **(C)** Immunofluorescence of PC3 cells transfected with shCtl or shYAP1, and treated with Rotenone (Rotenone, 5 mM). Cells were labeled with pericentrin (green) and Arl13b (red) along with DAPI (blue) (magnification: x60, scale bar 10 μ m). PC% indicates the percentage of primary cilium-positive (ciliated) cells, quantified by manual counting (n = 388 cells). **(D)** Flow cytometry analysis of TOMM20 expression. Left: Representative histograms of TOMM20 fluorescence intensity in (red) unlabelled PC3 cells, (blue) PC3 control (Ctl), (orange) PC3 cells transfected with siYAP1, (green) PC3 cells treated with metformin (Metf.), and (dark green) PC3 cells with combined siYAP1 and metformin treatment. Right: Quantification of mean fluorescence intensity (MFI) of TOMM20 expression across conditions. TOMM20, a mitochondrial outer membrane marker, was used to assess mitochondrial content or activity. Data are presented as mean \pm SD from at least three independent experiments. Statistical significance was determined using one-way ANOVA followed by Tukey's post hoc test (*p < 0.05 and ****p < 0.0001).

Figure S7. (A-F) Metabolic profiling using Omnilog in PC3 and NCI-H660 cells. Total cell growth was measured using MMP1 plates (Biolog), which assess the ability of cells to utilize specific carbon sources. The assay was performed in the presence of **(A)** glucose, **(B)** glucose-6-phosphate (G-6-P), **(C)** glucose-1-phosphate (G-1-P), **(D)** pyruvate, succinate, and **(E)** lactate. PC3 cells are shown in red and NCI-H660 cells in blue. The Omnilog system detects metabolic activity as a readout of overall cell proliferation on each substrate, revealing distinct substrate preferences between the two prostate cancer cell lines. **(G-N)** Mitochondrial substrate utilization profiling using Omnilog in PC3 and NCI-H660 cells. Cellular mitochondrial function was assessed using MITO S1 plates (Biolog), which measure the ability of mitochondria to utilize a single carbon source as the sole energy substrate. The assay included **(G)** citrate, **(H)** Cis Aconitate, glucose-1-phosphate (G-1-P), **(I)** Isocitrate, **(J)** α -Ketoglutarate, **(K)** succinate, **(L)** fumarate, **(M)** Malate and **(N)** Tryptamine. PC3 cells are shown in red and NCI-H660 cells in blue. Experiments were performed with n = 2 independent biological replicates. Statistical analysis was conducted using a two-way ANOVA.

Figure S8. (A) Heatmap showing the expression of selected AR marker genes in LNCaP and LNCaP-NE cells compared to NCI-H660. Gene expression was analyzed using Phantasus (v1.19.3). **(B)** Heatmap showing the expression of selected NE and PC marker genes in LNCaP cells compared to LNCaP-NE. Gene expression was analyzed using Phantasus (v1.19.3). **(C)** Heatmap showing the expression of selected NE and PC marker genes in LNCaP-NE cells compared to NCI-H660. Gene expression was analyzed using Phantasus (v1.19.3). **(D-H)** Heatmap showing the expression of selected **(D)** Mitochondrial complexes, **(E)** Mitochondrion, **(F)** Mitochondrial envelope, **(G)** Respirasome and **(H)** Inner mitochondrial membrane protein complex marker genes in LNCaP and LNCaP-NE cells compared to NCI-H660. Gene expression was analyzed using Phantasus (v1.19.3).

Figure S9. Integrated morpho-functional analysis of mitochondrial remodeling following long-term enzalutamide treatment. (A) Radar plot showing z-score-normalized mitochondrial morpho-functional parameters extracted using the EmitoMetrix pipeline from transmission electron microscopy images acquired at a spatial scale of 500 nm. Parameters describe mitochondrial size, shape, intensity distribution, and cristae orientation. Values

represent deviations from the global mean expressed in standard deviation units and enable comparison between control cells and cells treated with enzalutamide for 2 months. **(B)** SHAP (SHapley Additive exPlanations) summary plot illustrating the relative contribution of individual mitochondrial features to the prediction of the enzalutamide-treated condition. Each dot represents a single mitochondrion, with SHAP values indicating the impact of each feature on model output. Feature values are color-coded from low (blue) to high (red). Together, these analyses reveal a coordinated mitochondrial morpho-functional signature associated with long-term enzalutamide treatment.

Figure S10. (A–D) Heatmap analysis of gene expression before and after enzalutamide treatment in prostate cancer patients (GSE197780). Z-score normalized expression values are shown for patient samples collected before (orange bar) and after (green bar) enzalutamide treatment. **(A)** Expression of androgen receptor (AR) pathway markers and neuroendocrine prostate cancer (NEPC) markers. **(B)** Stratification of post-treatment samples into YAP1-high and YAP1-low groups using the median YAP1 expression value (7.79). Box-plot analysis compares NE marker expression using Welch’s t-test. NCAM1 was significantly higher in YAP1-high tumors ($p = 1.7 \times 10^{-5}$), ENO2 showed a borderline increase ($p = 0.050$), whereas CHGA, TP53 and MYCN showed no significant differences. **(C)** Expression of primary cilium-associated genes. **(D)** Expression of mitochondrial envelope-related genes. Each column represents an individual patient sample.

Figure S11. YAP1-expressing cells within NE-enriched clusters 8 and 11. **(A)** UMAP representation of cluster 8, highlighting the 7 YAP1-positive cells (red) among all cells in the cluster ($n = 1,324$). **(B)** Violin plot showing YAP1 expression levels in YAP1-positive versus YAP1-negative cells within cluster 8. **(C)** UMAP representation of cluster 11, highlighting the 5 YAP1-positive cells (red) among all cells in the cluster ($n = 482$). **(D)** Violin plot showing YAP1 expression levels in YAP1-positive versus YAP1-negative cells within cluster 11. **(E)** Expression of selected neuroendocrine markers (ASCL1, FOXA2, NKX2.1, MYCN, POU3F, INSM1, SIAH2, NCAM1, CHGA, CHGB, SYP and ENO2) in clusters 8 (blue) and 11 (pink) illustrating the range and heterogeneity of NE marker expression within these rare YAP1-expressing subsets.

All quantifications were performed using GraphPrism9 software. Statistical analysis: Two-way ANOVA; significant differences are indicated by **** $p < 0.0001$.

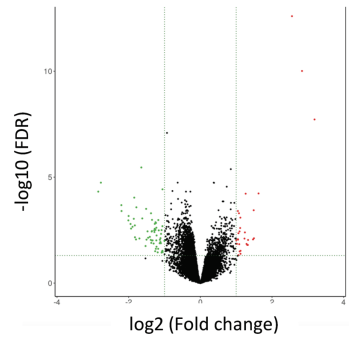
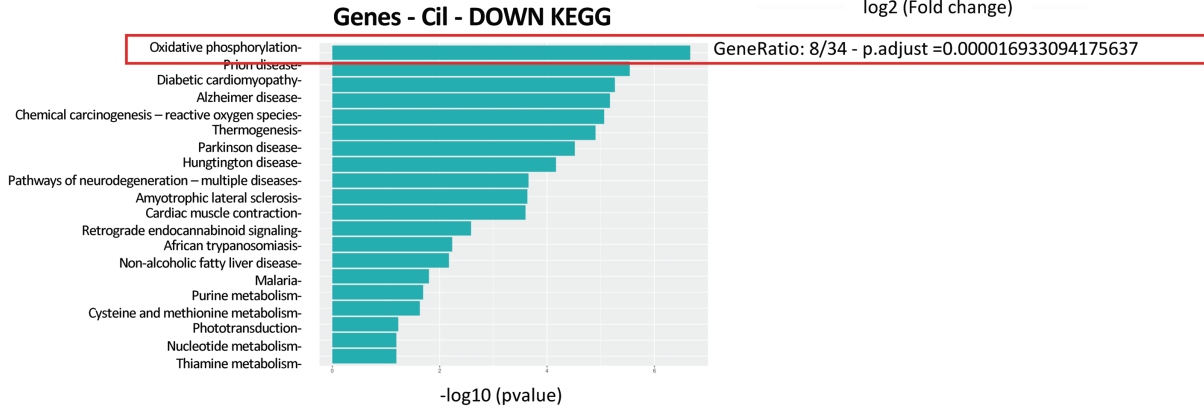
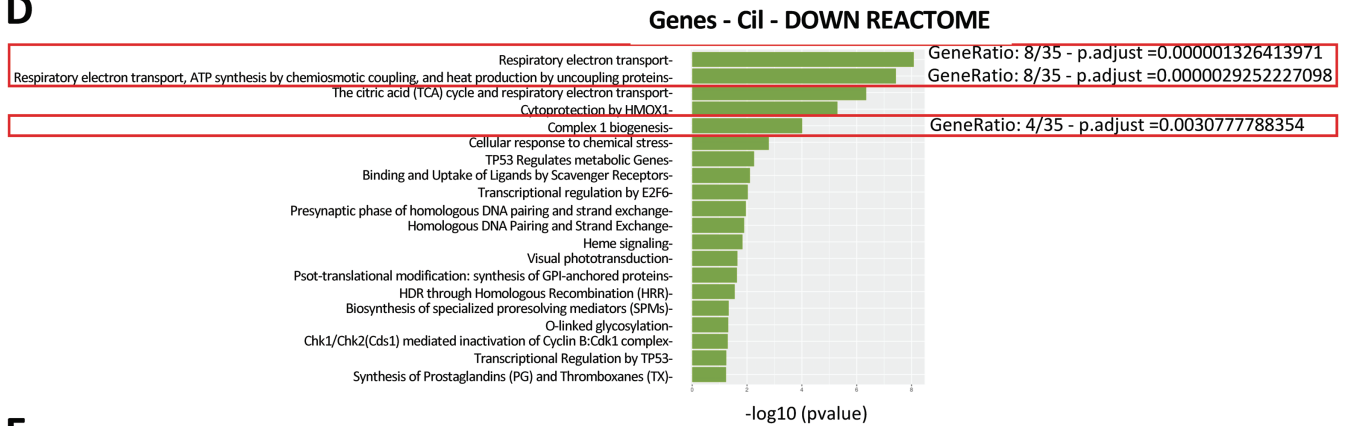
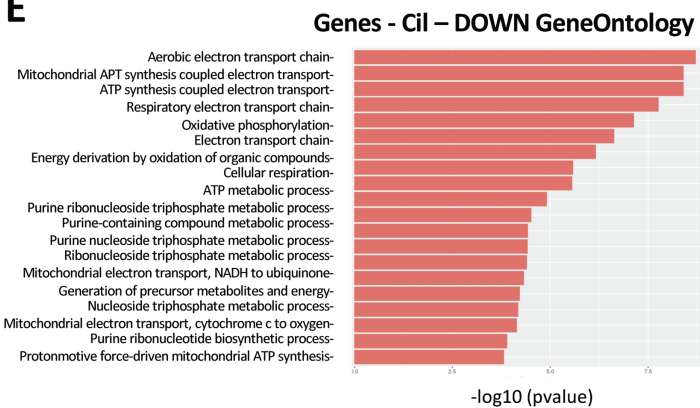
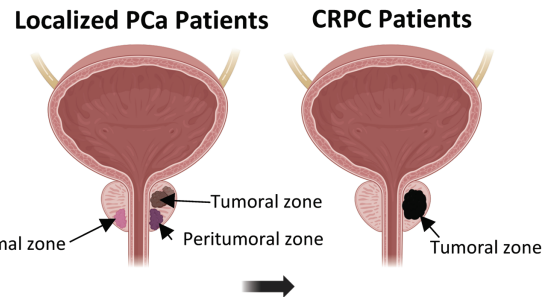
Figure S12. (A) Metabolic signature score based on the expression of *PFKFB3*, *LDHA*, *CA9*, and *MCT4* across all clusters identified by single-cell RNA-seq. Each bar represents the computed signature score for a given cluster. Clusters 8 (blue) and 11 (pink) are highlighted for emphasis.

A

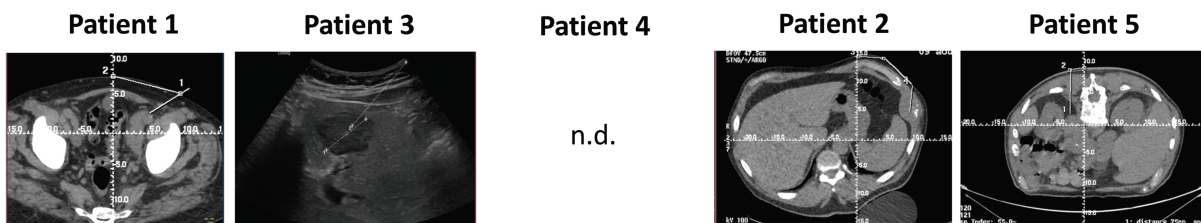
TCGA PRAD - Gleason score					
	6	7	8	9	10
GLI1-/IFT20-	32	143	39	61	2
GLI1-/IFT20+	4	49	14	29	0
GLI1+/IFT20-	10	41	10	33	2
GLI1+/IFT20+	0	14	1	14	0

B

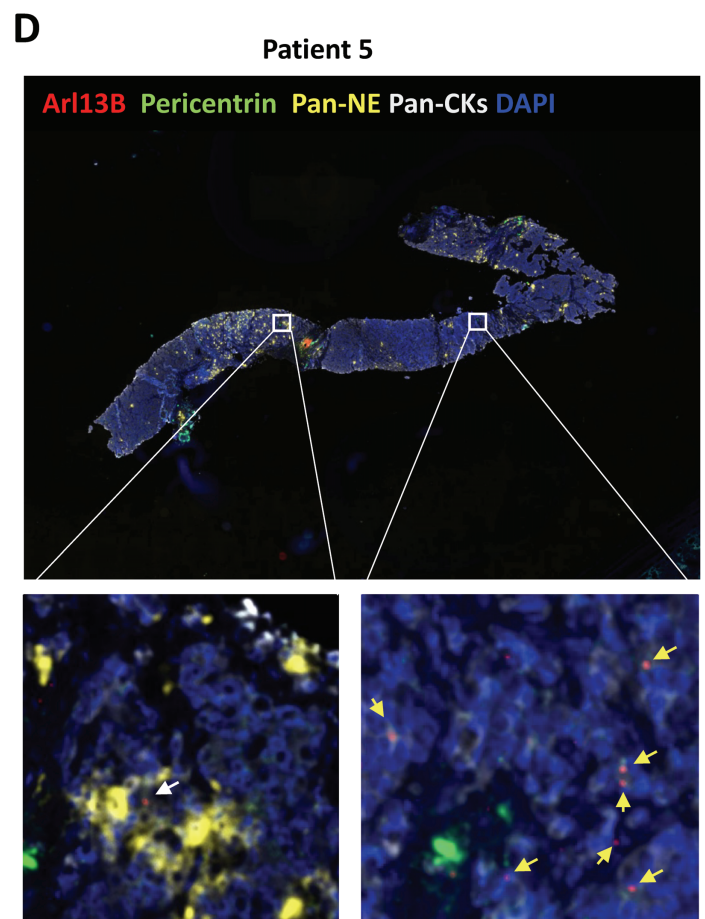
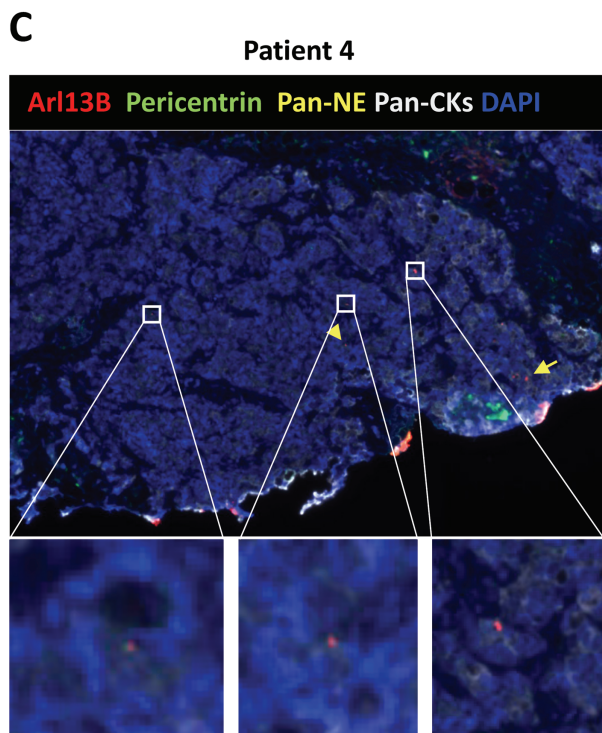
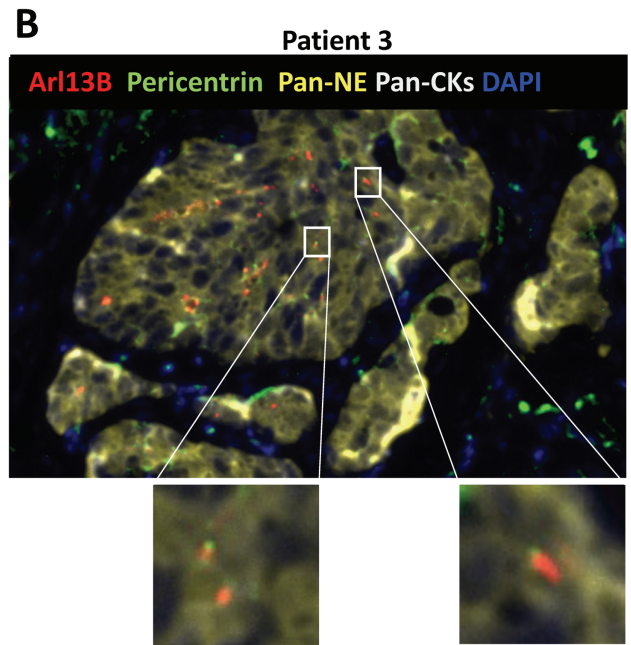
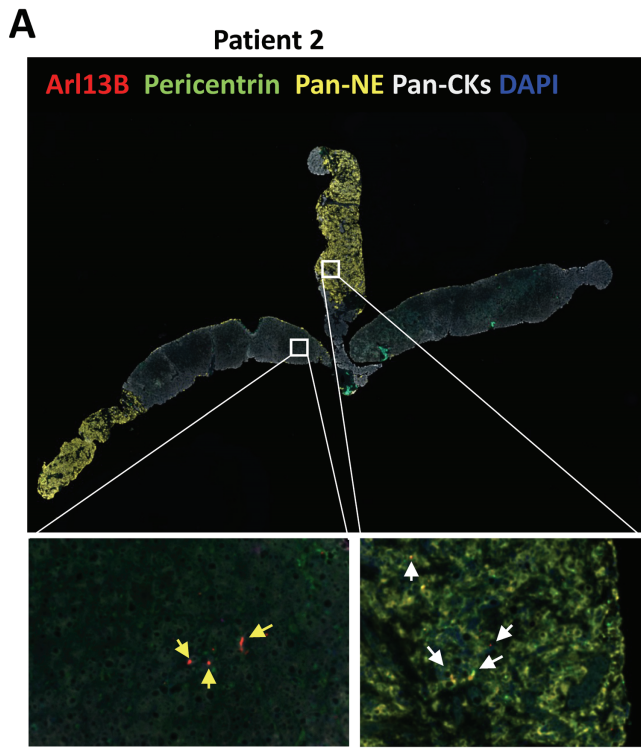
Differential expression analysis: Cilium/ No cilium

**C****D****E****F****G**

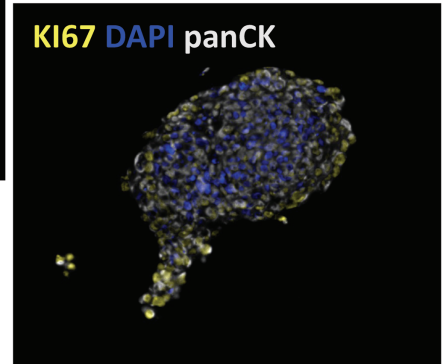
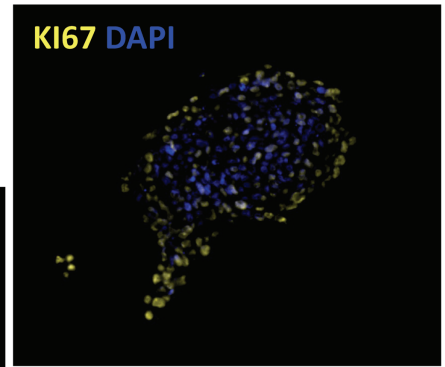
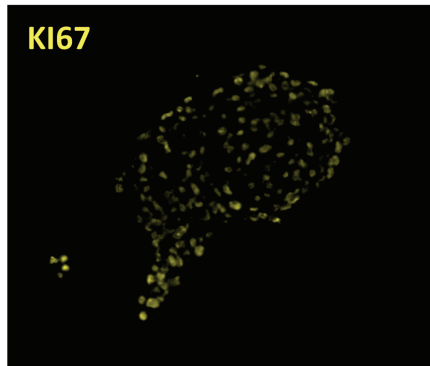
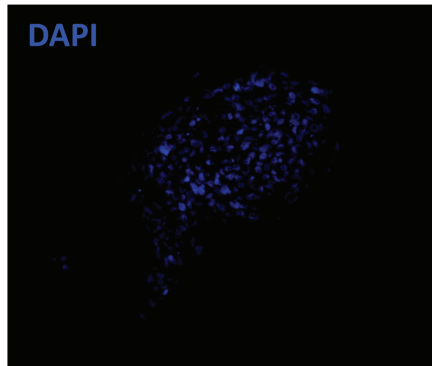
Antoine Lacassagne Cancer Center



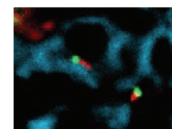
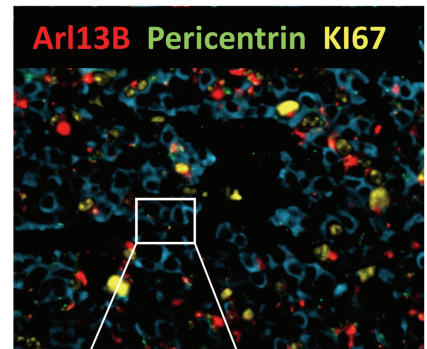
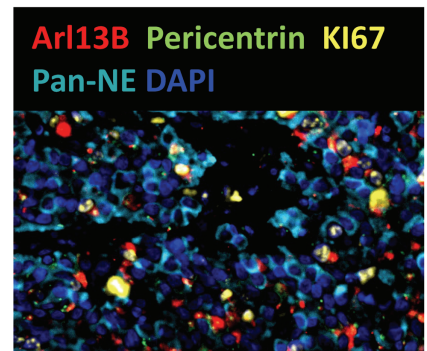
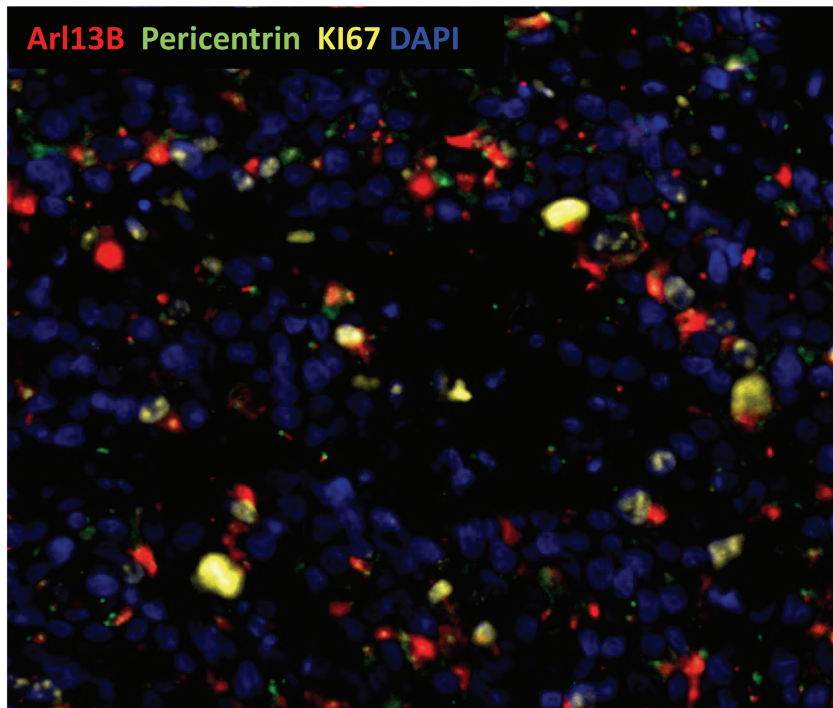
Data S1

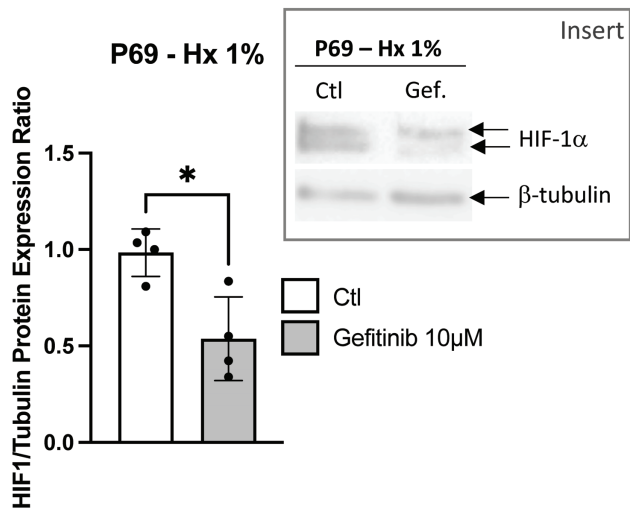
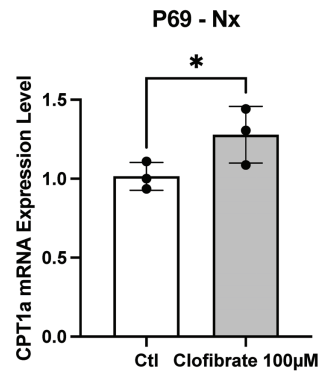
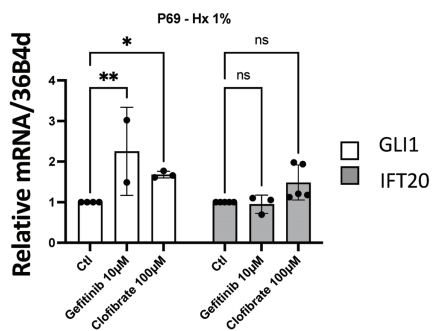
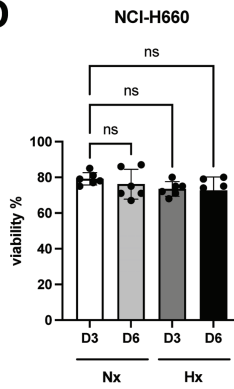
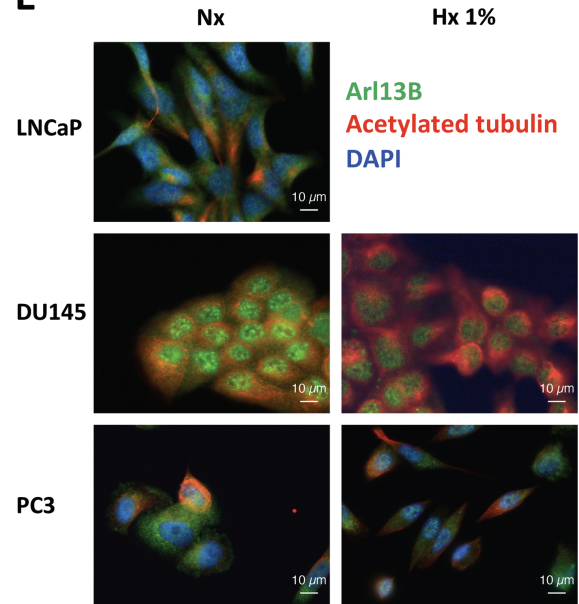
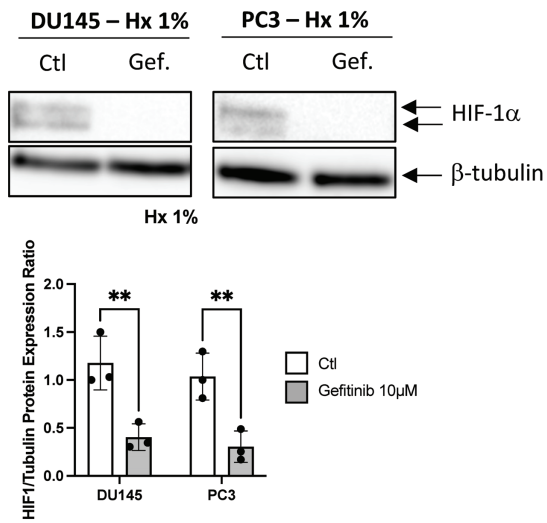
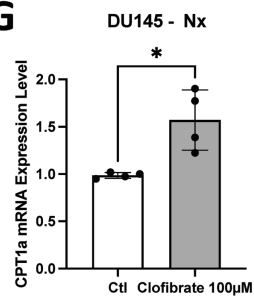
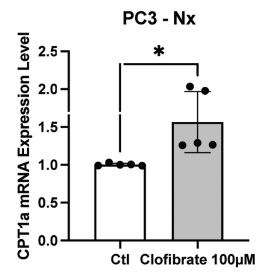
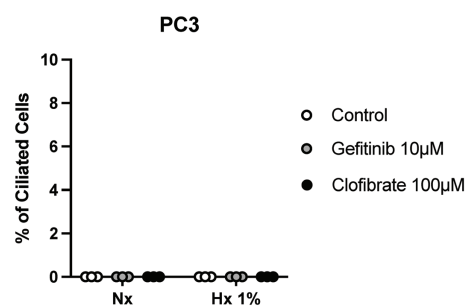


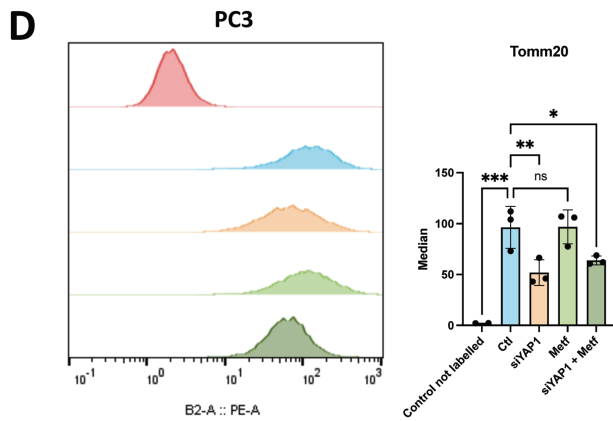
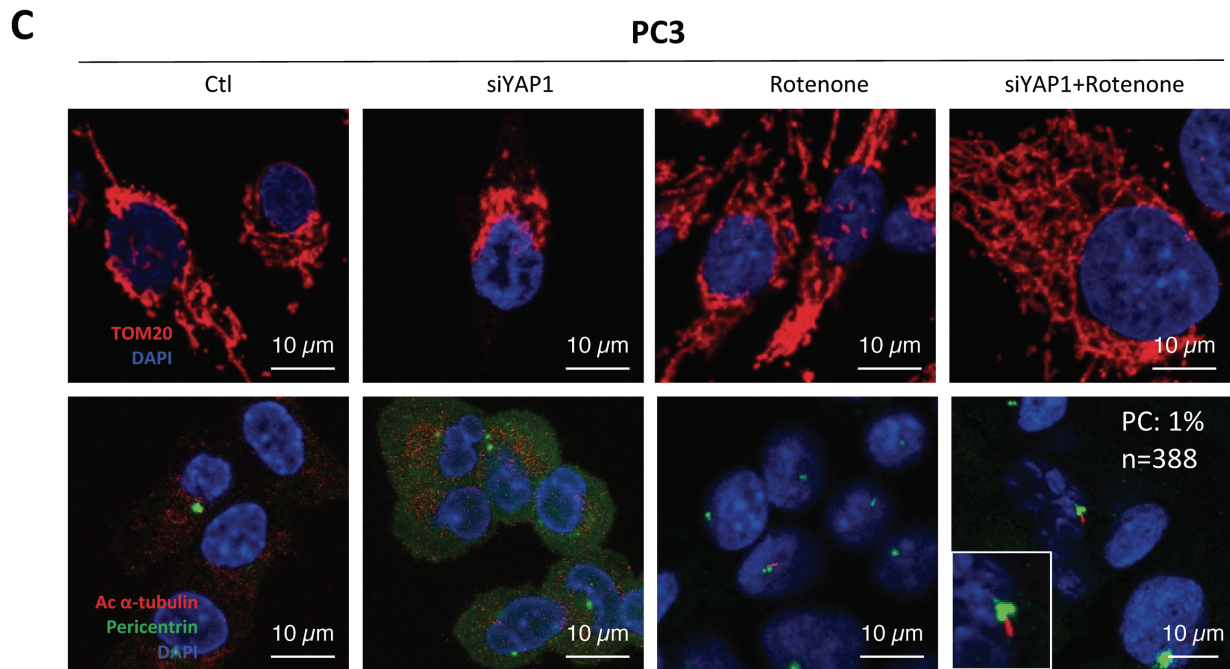
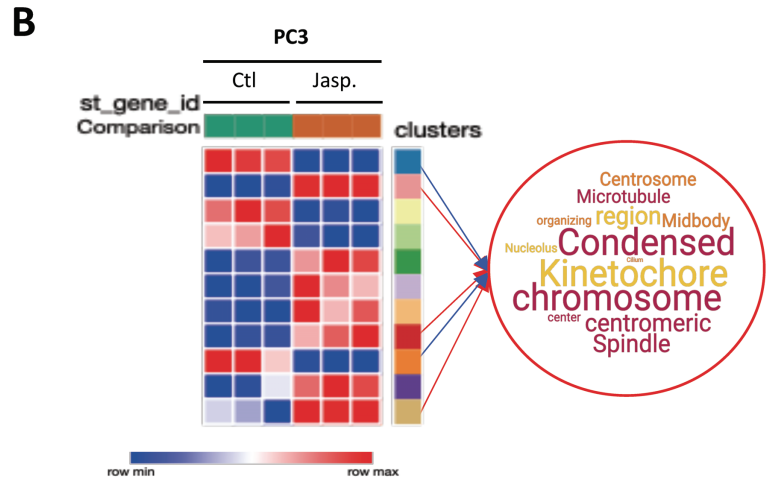
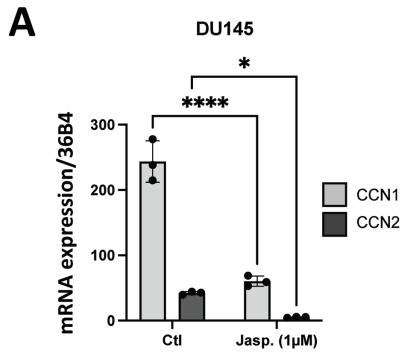
A

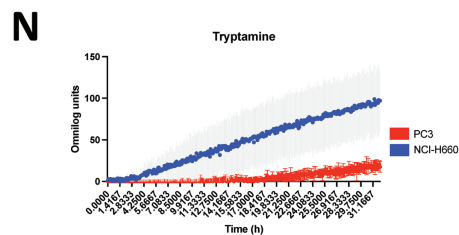
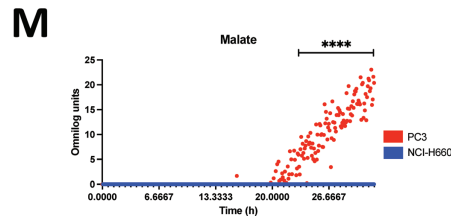
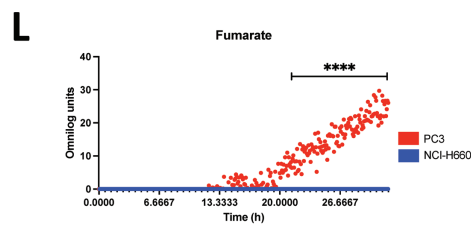
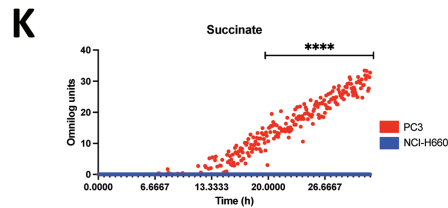
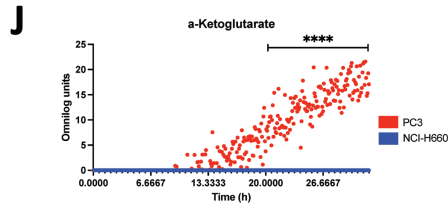
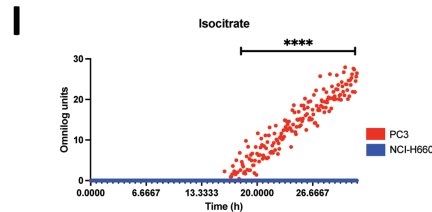
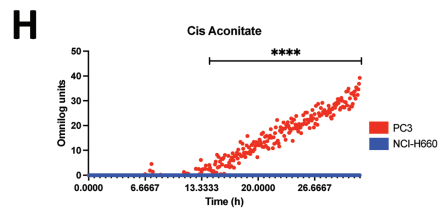
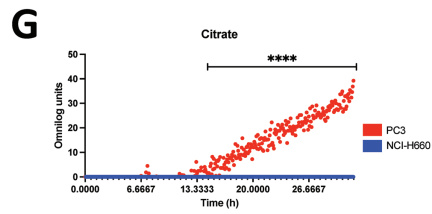
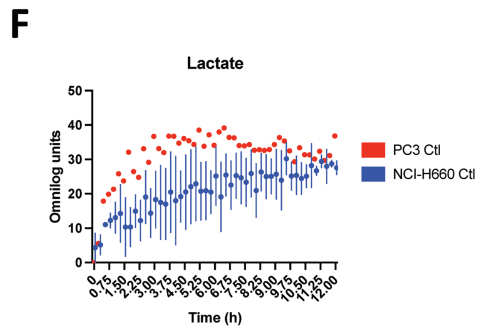
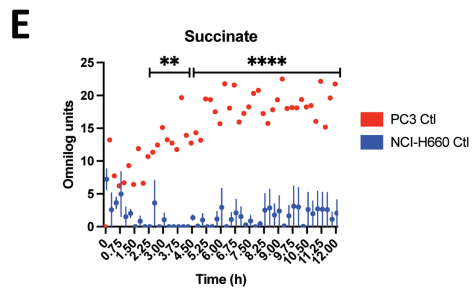
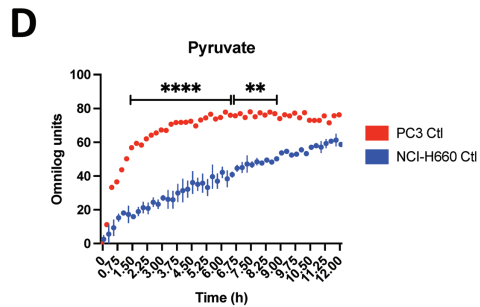
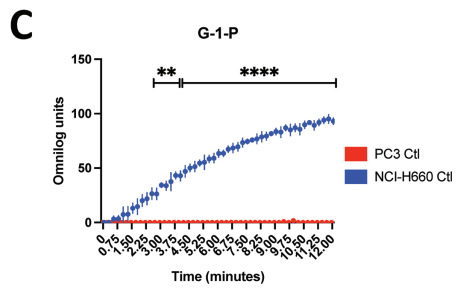
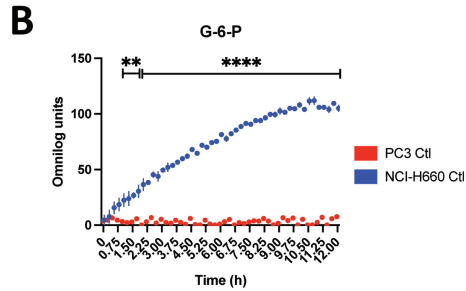
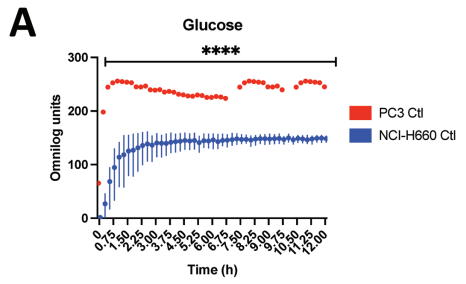


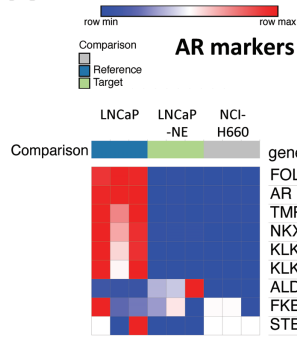
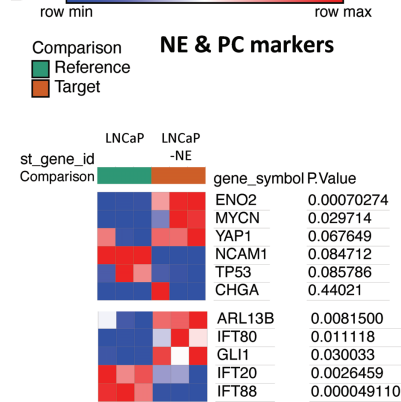
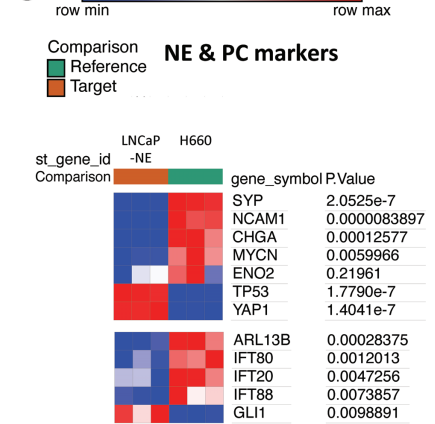
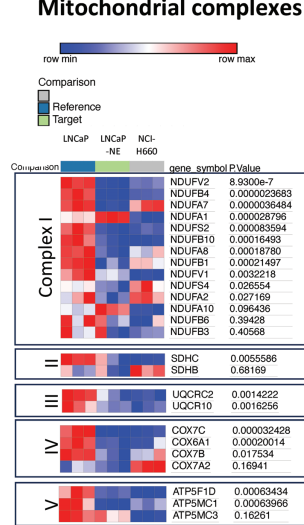
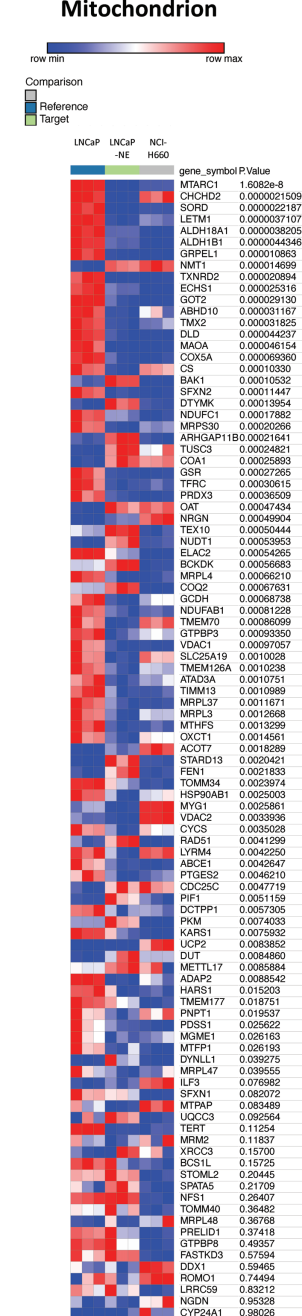
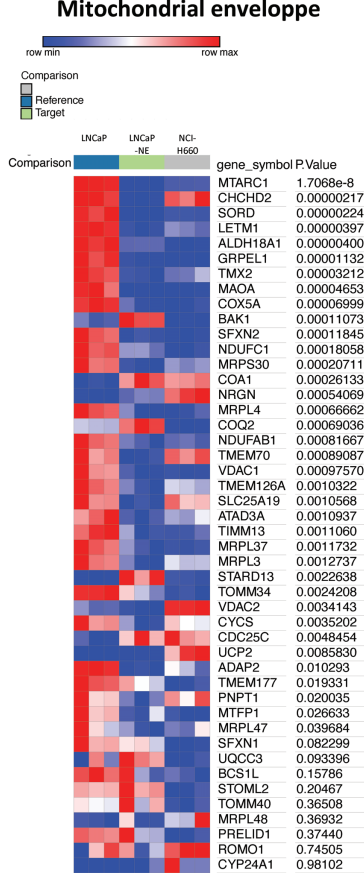
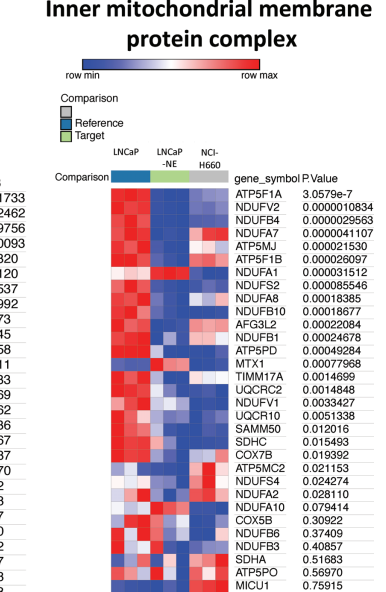
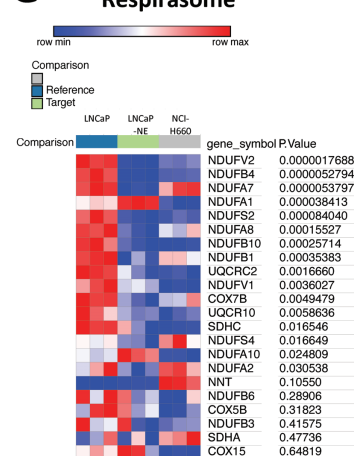
B

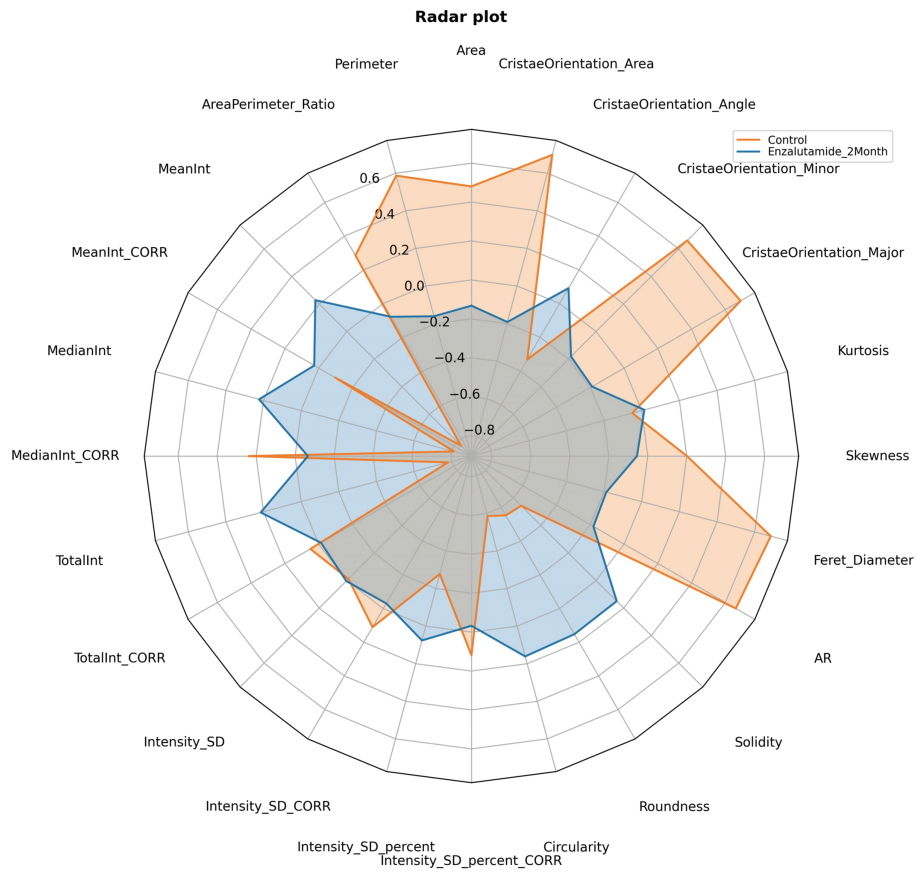
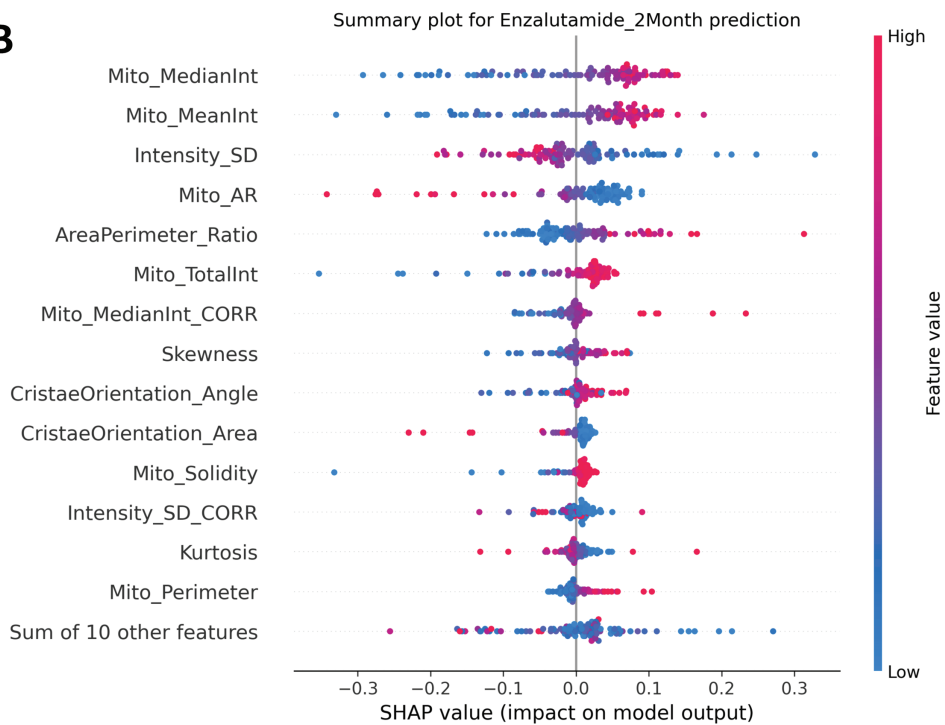


A**B****C****D****E****F****G****H****I****J****Data S4**

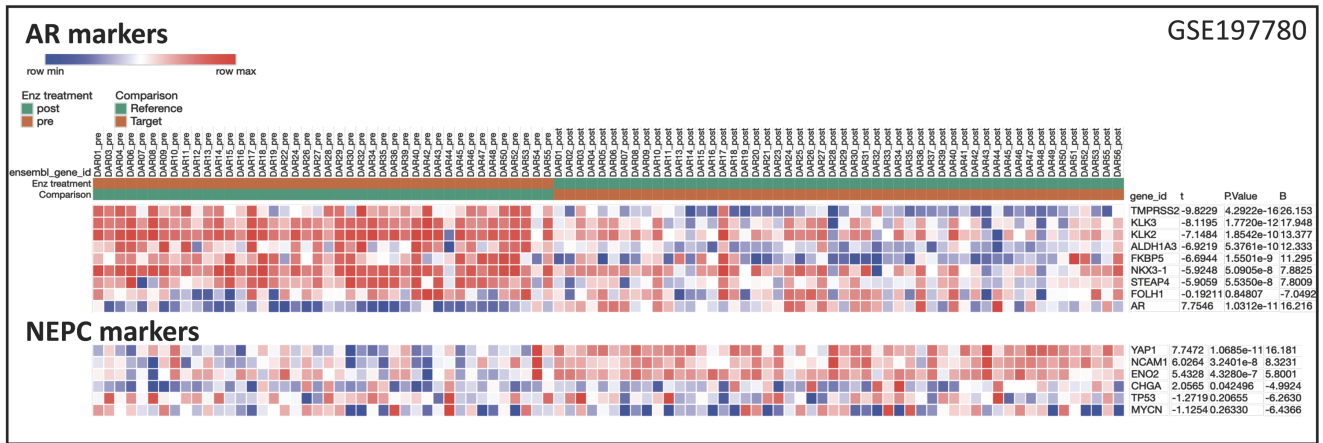




A**B****C****D****E****F****H****G**

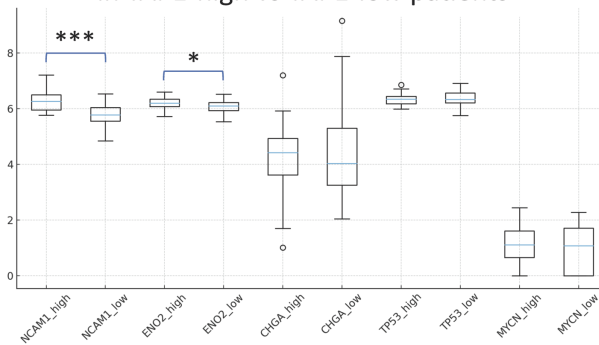
A**B**

A

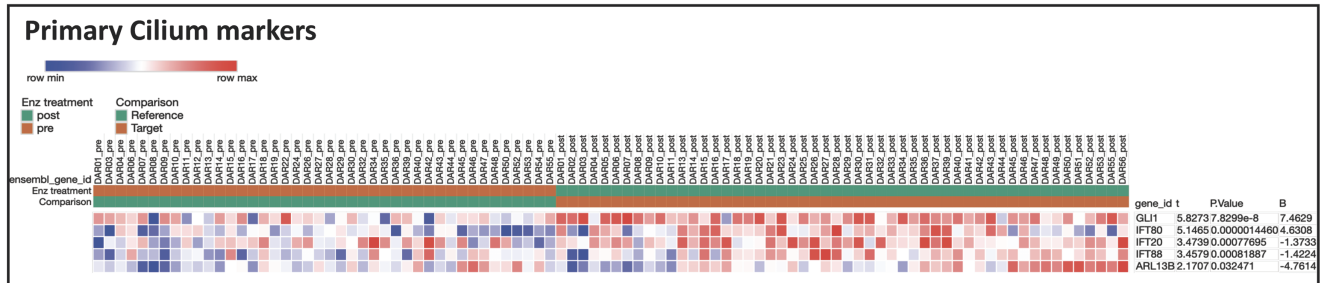


B

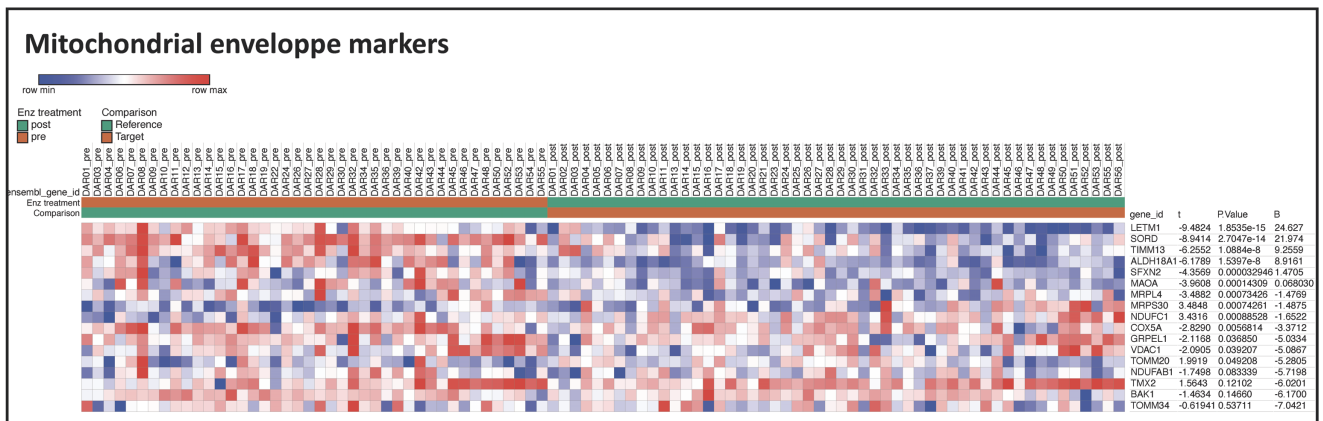
Expression of NE markers in YAP1-high vs YAP1-low patients

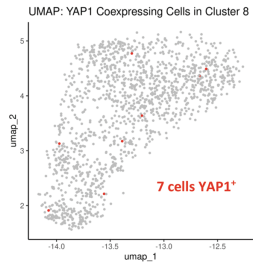
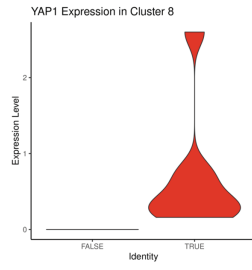
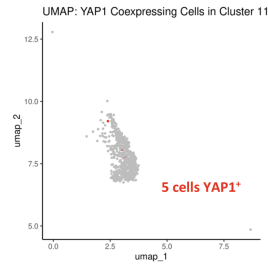
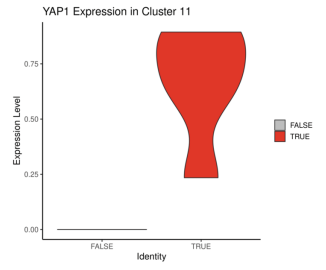
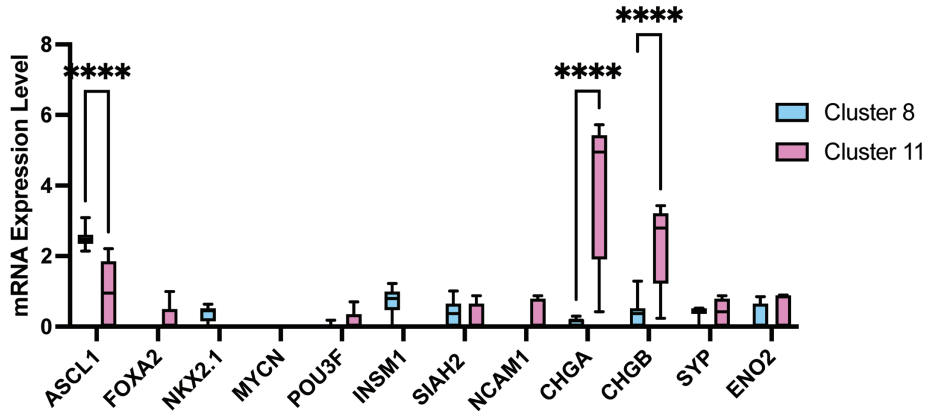


C



D



A**B****C****D****E**

A